Advanced Processing of Multiplatform Remote Sensing Imagery for the Monitoring of Coastal and Mountain Ecosystems

JAVIER MARCELLO[1], (Senior Member, IEEE), **FRANCISCO EUGENIO**[1], (Senior Member, IEEE), **CONSUELO GONZALO-MARTÍN**[2], **DIONISIO RODRÍGUEZ-ESPARRAGÓN**[1], **AND FERRAN MARQUÉS**[3], (Senior Member, IEEE)

[1]Instituto de Oceanografía y Cambio Global, IOCAG, Unidad Asociada ULPGC-CSIC, 35017 Las Palmas de Gran Canaria, Spain
[2]Department of Computer Architecture and Technology, Universidad Politécnica de Madrid, 28660 Madrid, Spain
[3]Signal Theory and Communications Department, Universitat Politècnica de Catalunya BarcelonaTECH, 08034 Barcelona, Spain

Corresponding author: Javier Marcello (javier.marcello@ulpgc.es)

ABSTRACT Coastal areas are key to sustaining biodiversity, but their complexity and variability makes their analysis challenging. On the other hand, mountain ecosystems include a large percentage of the global biodiversity and their monitoring is essential, as they are especially vulnerable to climate change. In this context, remote sensing offers a cost-effective technology for the conservation of both kinds of natural areas. In this work, multispectral and hyperspectral data recorded by sensors, onboard satellites, aircrafts and remotely piloted aircraft systems (RPAS), have been used for the sustainable management of natural resources. Specifically, a multiplatform methodology has been developed to process multisensor high spatial resolution imagery and the main benefits and drawbacks of each technology have been identified. Advanced processing techniques in each stage of the methodology have been selected to provide accurate and validated benthic and vegetation maps. Two challenging ecosystems, located in Cabrera and Teide National Parks, have been selected for this study. They correspond with a coastal and a mountain island ecosystem, respectively. To address the associated challenges, the use of imagery with the maximum spatial and spectral resolution, provided by Sentinel-2, WorldView-2, CASI and Pika-L, has been considered. Results have been validated with in-situ data and by the National Parks' managers and they have shown the ability of remote sensing to accurately map both Parks when the appropriate imagery and techniques are selected. The best performance was achieved with the Support Vector Machine classifier and, in general, WorldView can be considered the most appropriate platform when factoring in cost, coverage and accuracy.

INDEX TERMS Benthic mapping, multispectral and hyperspectral imagery, remote sensing, vegetation mapping.

I. INTRODUCTION

According to the United Nations Environmental Programme and its digital update of September 2020 [1], in the last few years, terrestrial coverage of protected areas increased to 15.0% while the marine coverage increased further to 17.3% in national waters. In Spain, specifically, protected areas cover over 27% of its total surface, with preserved marine regions exceeding 8% of its total surface and with a coastline length about 7,880 km [2]. These areas are essential for the conservation of biodiversity as well as provide services to society. Moreover, activities around visitors are a source of "green" jobs. As an example, Spanish Parks receive over 21 million visitors yearly. However, to reach their full potential and their efficient management, adequate mechanisms for the monitoring and evaluation are necessary [3].

Mountain ecosystems cover a quarter of the land area. They are challenging environments to monitor due to relevant topographic and climatic gradients. Coastal areas

The associate editor coordinating the review of this manuscript and approving it for publication was Stefania Bonafoni.

are also inherently difficult to supervise because of their variability and complexity. In this context, high resolution satellite-based imaging systems, with spectral bands within the visible and near infrared spectrum, can provide information of coastal parameters and land covers at broader spatial and finer temporal scales than those achieved through field observations alone.

Nevertheless, geometric distortions, as well as radiometric, atmospheric and solar effects have high impact on the results [4]–[7].

Multispectral (MS) satellite sensors have been used for many decades, however, more recently, hyperspectral (HS) imagery has been considered to map vegetation or benthic habitats at high resolution [8]–[15]. Unfortunately, high spatial HS sensors onboard satellites are not available nowadays and, as a result, airborne or RPAS HS instruments are the only options to map complex habitats environments at the maximum spatial and spectral resolutions.

Given the enormous potential of remote sensing systems for environmental conservation [16], this work focuses on developing a multisensor methodology that, applied to multispectral and hyperspectral imagery, can allow the sustainable management of natural resources. A complete processing protocol has been developed for monitoring coastal shallow-waters and mountain environments, and their critical elements have been explored. Contributions are presented regarding the best advanced correction and classification techniques, as well as a comparative assessment of the benefits of using the latest satellite multispectral and airborne/RPAS hyperspectral high resolution imagery to obtain accurate maps. In coastal ecosystems, the outcome focuses mainly on detecting and classifying seagrass meadows in waters up to 30m deep, like *Posidonia* and *Cymodocea* in the coastal ecosystem. In land areas, the goal is to map endemic and invasive vegetation species in order to analyze their distribution, health and dynamics.

To develop and validate the proposed techniques, two representative areas have been studied: Teide and Cabrera National Parks, located in the Canary and Balearic archipelagos (Spain), respectively. Island ecosystems have been selected because of their complexity and richness in endemic species and because they are most vulnerable to climate change, tourism and the introduction of exotic species. Furthermore, Park managers lacked updated and high resolution maps of their protected natural areas.

II. MATERIAL AND METHODS

A. STUDY AREAS

The Cabrera and the Teide National Parks are located in the Balearic Islands (Mediterranean Sea) and the Canary Islands (northwest African coast), respectively, as shown in Fig. 1(a).

The Cabrera Archipelago, made up of 19 islands or islets and located just 15 kilometers from the south coast of Mallorca, is the best example of undisturbed ecosystems in the Spanish Mediterranean area. Due to its isolation,

Cabrera has great natural value and it is frequently considered one of the best preserved ecosystems in Spain as well as the Mediterranean. Seagrass meadows, specially, are one of the archipelago's most important benthic habitats, with *Posidonia oceanica* as the dominant species, which it is protected by various regional, national and European regulations [17]. Within the framework of this research, a detailed study of *Posidonia* has been carried out through the use of high resolution MS and HS remote sensing data. Fig. 1(b) shows a picture of areas taken during the 2018 RPAS and field campaigns.

The Canary Islands, thanks to the great variety of endemic species, are one of the most important spots of biodiversity in Europe. The Teide National Park, located in Tenerife Island, is an important natural areas of Canary Islands. The Teide peak, formed by several overlapping volcanoes, is Spain's highest mountain (3718 m). The vegetation of this ecosystem is a characteristic shrubland of the high Mediterranean mountain, but it incorporates elements of great physiognomic originality. The most characteristics species are *Pinus canariensis* (canarian pine), *Spartocytisus supranubius* (Teide broom), *Descurainia bourgaeana* (Teide flixweed), *Pterocephalus lasiospermus* (summit rosebush), *Aenocarpus viscosus* (Canary Island flatpod), and *Echium wildpretii* and *Echium auberianum* (Mount Teide bugloss) [18]. Fig. 1(c) identifies the most abundant species of the Park and highlights the ecosystem's heterogeneity and complexity.

B. DATA

The satellite data used come from WorldView-2 (WV-2) and Sentinel-2 (S-2) multispectral sensors. Acquisition dates were planned or chosen to match the hyperspectral airborne/RPAS overflights. Table 1 presents the spatial and spectral characteristics of the remote sensing data used in the study.

TABLE 1. Technical characteristics of the multispectral and hyperspectral imagery.

| Platform Sensor	Spatial Resolution (m)	Number of Spectral Bands	Wavelength range (nm)	Bandwidth range (nm)
Sentinel-2 MSI	10, 20 and 60	13	430 - 2280	15 - 115
WorldView-2	2	8	400 – 1040	37 - 99
Casa C-212 CASI-1500i	0.75	68	380 – 1050	3
Dji Matrice 600 Pika-L	0.10	120	400 - 1000	4

Table 2 lists the specific scenes selected for each location. For the Cabrera National Park, three different platforms were analyzed: Sentinel-2 and WorldView-2 satellites as well as the DJI Matrice 600 RPAS equipped with the Pika-L instrument. For the Teide National Park, three different platforms were also used: WorldView-2, the airborne CASI

(a)
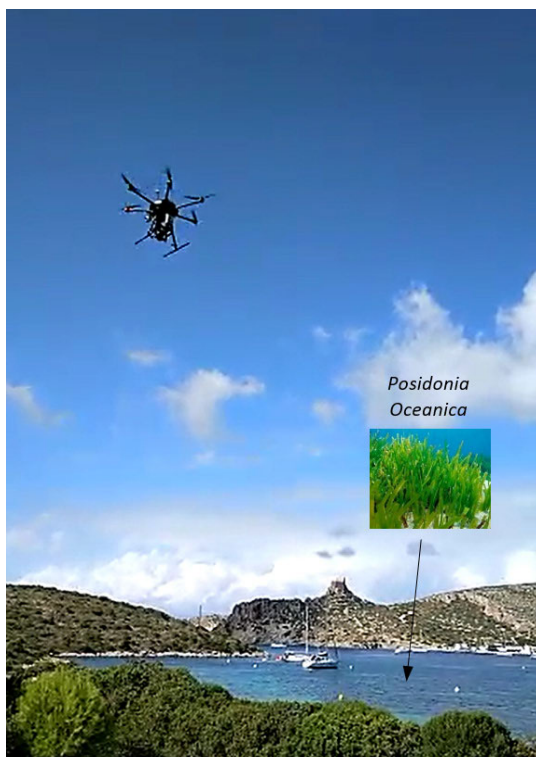
(b)
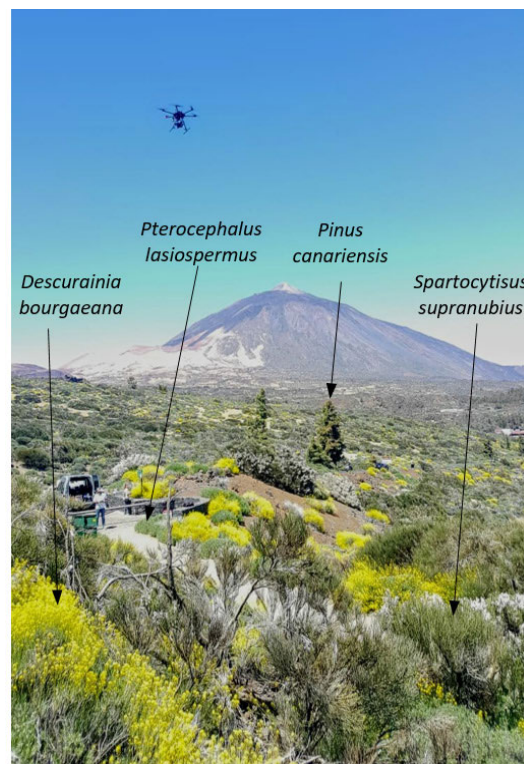
(c)

FIGURE 1. Areas studied: (a) Balearic islands and canary islands geographic location (OpenStreetMap©). RPAS campaigns during 2018: (b) Cabrera national park and (c) Teide national park.

sensor and the Pika-L camera. Sentinel-2 was not used because a 10 m pixel size is not enough to discriminate the small and mixed shrubs.

Fig. 2 shows the specific areas sensed by each platform, as well as the color composite images of each sensor, for a small subset of the scene, to better appreciate differences in spatial resolution.

The trade-off between coverage and spatial resolution is evident. It is important to point out the importance of selecting the right date for the Teide Park. Specifically,

the end of the spring season was chosen, as the discrimination capability is highest during the blooming stage of some plant species. For this reason, along with the National Park authorities, all images were recorded on May 31st or June 1st.

In-situ field data was acquired simultaneously with the aircraft and RPAS campaigns to train and test the processing methodology. Accurate sampling was performed in many locations to cover each species' variability, and reflectance measurements were recorded in the visible and near-infrared range of the spectrum (350–2500 nm) over
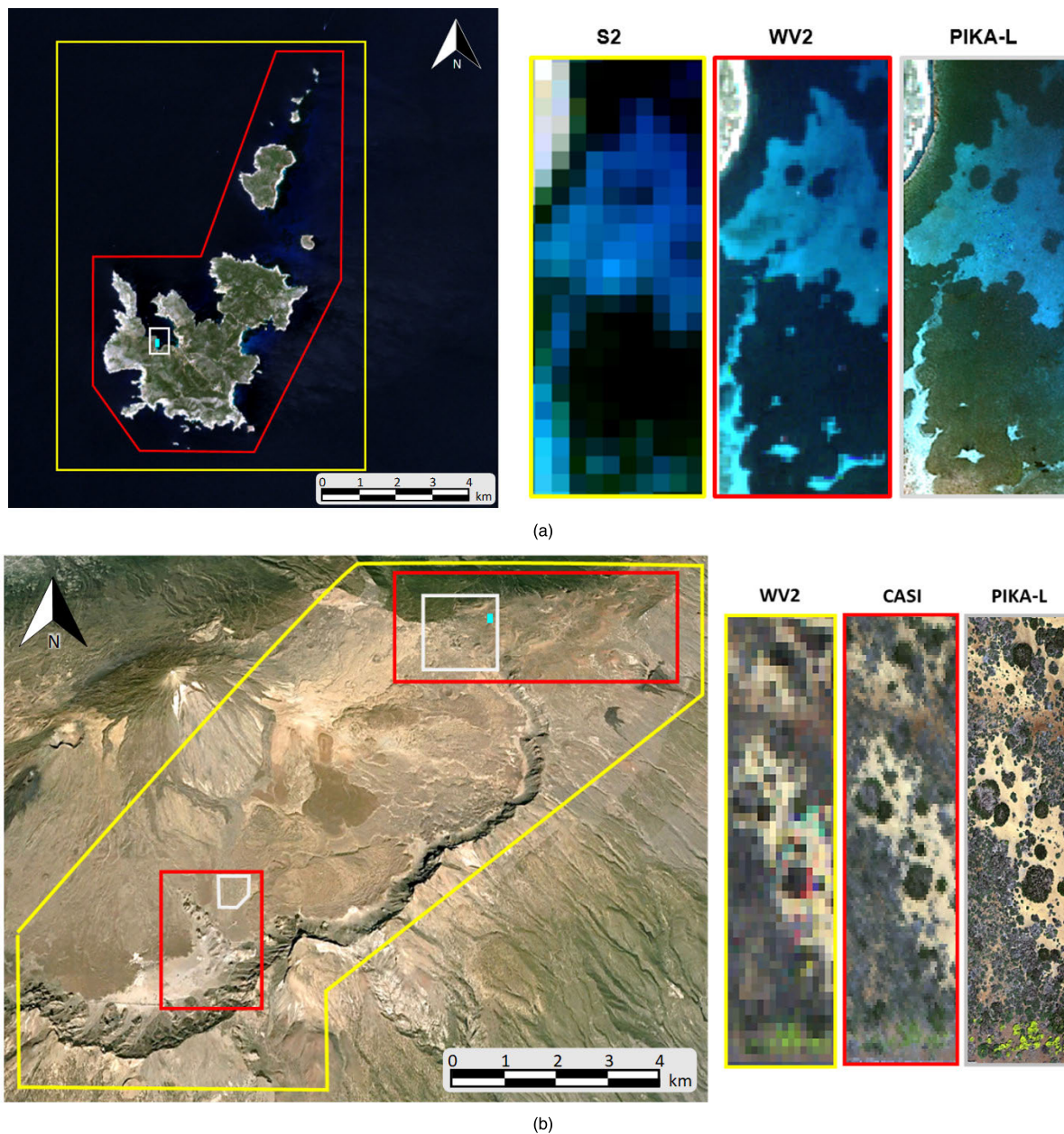
FIGURE 2. Coverage of the multiplatform remote sensing scenes and true color composite images for the subset marked in cyan: (a) Cabrera national park (S-2 in yellow, WV-2 in red and Pika-L in gray) and (b) Teide national Park (WV-2 in yellow, CASI in red and Pika-L in gray).

**TABLE 2.** Scenes used in the analysis of both national parks.

National Park	Sensor	Date	Time (UTC)
Cabrera	Sentinel-2	September 30th, 2018	10:40 hr
	Worldview-2	September 1st, 2016	10:29 hr
	Pika-L	September 18th, 2018	14:00 hr
Teide	Worldview-2	June 1st, 2018	12:05 hr
	CASI	June 1st, 2017	11:00 hr
	Pika-L	May 31st, 2018	12:30 hr

homogeneous and flat areas using the ASD FieldSpec-3 field spectroradiometer.

C. PROCESSING METHODOLOGY FOR COASTAL AREAS

The development of new Earth observation platforms and advanced imagery sensors, with improved capabilities, can assist in the generation of accurate knowledge for the sustainable management of natural resources in littoral zones. In this context, the overall methodology for the selected vulnerable ecosystem, Cabrera National Park, is shown in Fig. 3. The goal is to discriminate the following benthic classes: seagrass (*Posidonia* or *Cymodocea*), sand or sediments, and rocks.

A preliminary pre-processing is applied to obtain corrected and masked imagery. Regarding atmospheric correction, for the Pika-L scene, the RPAS carries a radiometer that points to
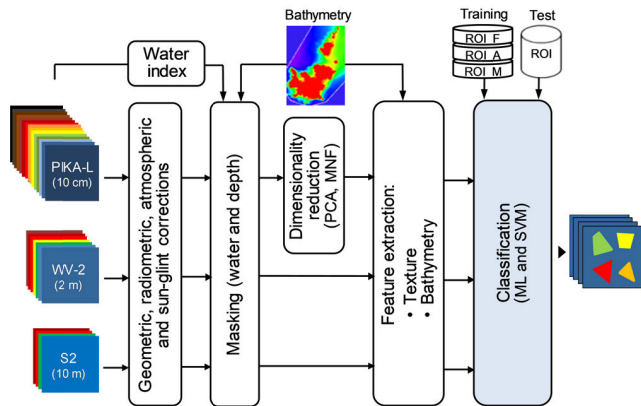
FIGURE 3. Overall processing methodology to generate the seafloor maps from multiplatform HS and MS imagery.

On the other hand, SVM can perform well, even when a large training set is not available. According to literature and different experiments, the Gaussian radial basis function kernel has been used and grid search was used to find the optimal parameters [5], [26], [27].

In this work, 3 different types of training regions of interest (ROIs) were set up depending on the amount of pixels used to train the classifiers (ROI_F: ROIs with few pixels, ROI_A: ROIs with medium amount of pixels and ROI_M: ROIs with many pixels). For each category (ROI_F, ROI_A and ROI_M), 6 different ROIs datasets were created selecting pixels at different regions and depths to deal with the variability of each class. The same regions were chosen for all the sensors, thus, the number of pixels for each type of ROI depends on the sensor spatial resolution. As a reference, for a 2 m sensor, the approximate number of pixels were 20 for ROI-F, 200 for ROI-A and 2000 for ROI-M.

the zenith calculating the total irradiance in the 400–1000 nm range. The reflectivity is computed with the simultaneously sensed information of the radiance and irradiance. For the WorldView-2 data, the FLAASH advanced atmospheric model-based algorithm has been applied as it achieves excellent performance for coastal areas [6]. For Sentinel-2, the atmospheric correction method to derive the reflectance images is Sen2Cor [19], a combination of state-of-the-art methods adapted to S-2. Afterwards, non-water areas are masked using a normalized water index that considers the blue and near-IR channels. In addition, when the sea surface was not calm, a sun-glint correction was applied [20], [21]. Finally, using bathymetric information, water areas over 30 m deep were removed from the analysis because the water column attenuates the optical channels and radiation cannot reach the seafloor from a certain depth.
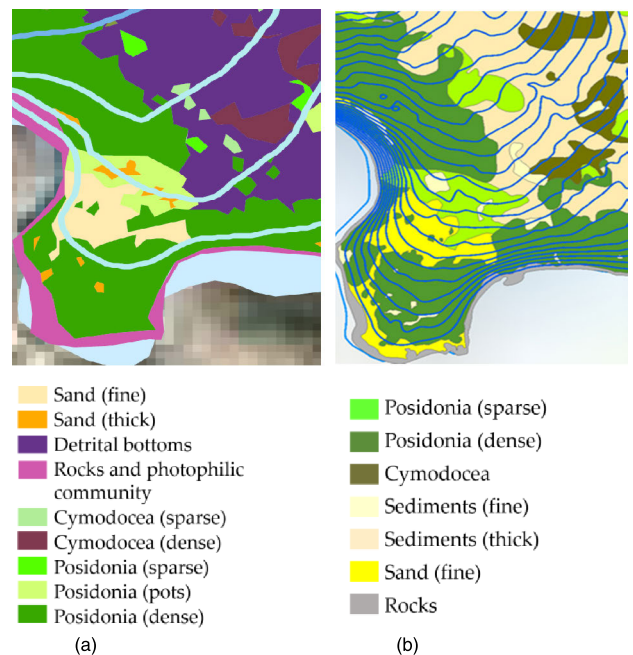
For the hyperspectral image, Principal Component Analysis (PCA) and Minimum Noise Fraction (MNF) have been considered due to their ability to extract the relevant information in a reduced number of components [22]. After visual inspection, the first 5 components have been selected in the experiments.

When corrections were performed, feature extraction was undertaken to get additional information to improve the classifiers' accuracy. Texture information (mean and variance), calculated applying the co-ocurrence matrix [23] to the blue band, was added into the classifier to increase the discrimination capability between classes. Bathymetry [24] was also used as an additional feature to improve the generation of benthic maps.

Finally, Support Vector Machine (SVM) and Maximum Likelihood (ML) supervised classifiers were used, as they provide greater performance in seabed mapping than other tested algorithms like Spectral Angle Mapper (SAM) [5]. Support Vector Machine is a machine learning technique that has demonstrated excellent robustness and accuracy when compared to other advanced methods (deep convolutional neural networks, random forests, sparse representation-based techniques, logistic regression-based algorithms, etc.) [25].


FIGURE 4. Reference benthic maps: (a) Posidonia project; (b) Cabrera national park.

Finally, the mapping accuracy was computed using an independent dataset of test regions. The confusion matrix and the Kappa coefficient were used during the assessment [28]. Basically, the confusion matrix represents true classes versus the classifier's predictions, with the overall accuracy parameter measuring the correctly classified pixels. The Kappa index measures the agreement between classification and truth values, but taking into account the agreement occurring by chance. Visual analysis was also conducted using the available benthic maps of the area (Fig. 4): Life Posidonia Project of 2005 [29] and Cabrera National Park of 2011 [24]). Unfortunately, these maps are not updated as it is a labor intensive task that requires an important financial investment.

D. PROCESSING METHODOLOGY FOR LAND AREAS

The monitoring of the Teide Park follows a similar methodology (corrections, feature extraction and classification steps). Fig. 5 shows the simplified flowchart.
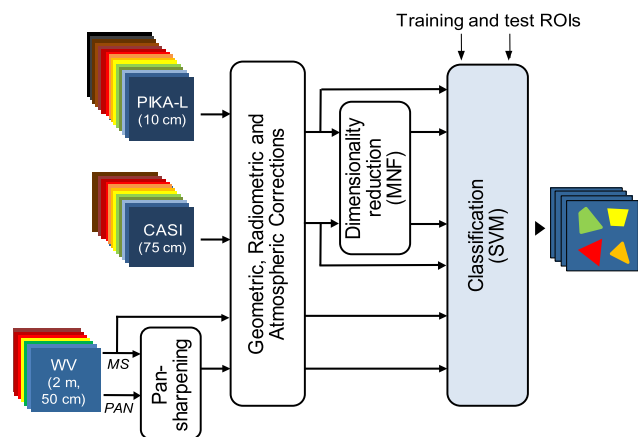
FIGURE 5. Processing methodology for the monitoring of land ecosystems with multiplatform data.

Preprocessing tasks are similar to those of the coastal methodology. The main difference in WV-2 for land applications is the possibility to apply pansharpening techniques [30]–[33] to increase the spatial resolution by a factor of 4. These techniques cannot be used to map the seafloor as the panchromatic image integrates a wide spectral range and, therefore, only provides bottom information for extremely shallow waters. The Gram-Schmidt algorithm [34] has been used as it provides excellent performance, increasing the spatial detail with low spectral distortion. FLAASH [35] was also applied for the atmospheric correction when introducing the appropriate parameters [36].

For the HS data, the high number of spectral channels turns into a decrease on the classifier's performance if the size of the training dataset is not large enough with respect to the number of bands. To solve this 'Hughes' phenomenon [37], dimensionality reduction techniques can be applied. In this work, after the preliminary assessment for the CASI sensor [38], the Minimum Noise Fraction transform (MNF) was chosen to remove redundant information.

Training and testing samples for the classification were collected over two campaigns locating, accurately and randomly, field data for each vegetation species to be analyzed (*D. bourgaeana, S. supranubius, P. canariensis* and *P. lasiospermus*). Plants with different sizes and blooming stages were selected to take into account the variability of each species throughout the Park. The SVM classifier was chosen because of its robustness to the quality and quantity of the training dataset and because it performs much better than the ML for land applications [10]. Before applying the classifier, the Jeffries-Matusita distance was calculated on the training pixels to analyze the separability of each vegetation class. This distance ranges from 0 to 2, being 2 a perfect separability value between classes.

III. RESULTS

The following sections present the results for the ecosystems selected. Processing has been carried out using ENVI 5.2.

A. COASTAL SHALLOW WATERS

The main results for the mapping of benthic habitats in Cabrera are next presented. Maps have been generated for the complete scene of each sensor (Fig. 2(a)), but only the common area was considered for the comparative assessment. Fig. 6 includes the imagery used in the analysis. Differences in spatial resolution between sensors are evident. Noisy areas in the upper-left corner of the RPAS image can be appreciated due to problems during the acquisition.

To check the effects of the spatial resolution in the mapping results, the Pika-L image was also resized to 2 m applying a bilinear resampling algorithm. To better understand the complexity of the mapping, 1 m isobaths are also included in the figure.

As indicated, 3 different categories of training regions of interest (ROIs), each one with 6 datasets, were considered to train the classifiers. In this context, Fig. 6(f) presents the example of one training dataset. *Posidonia/Cymodocea* is displayed in green while sand and rocks are highlighted in yellow and brown, respectively. It can be appreciated that training regions are selected to cover the variability of the classes and, when possible, at different water depths.

Table 3 shows the overall accuracy of the benthic maps generated by ML and SVM classifiers. Mean and standard deviation values are included. For the hyperspectral imagery, results using dimensionality reduction techniques (PCA and MNF transforms) have also been tested. After visual inspection, the first 5 components were selected as the remaining channels were mainly noise. Besides, to assess if using the 8 bands of WV-2 improves accuracy, experiments removing the 4 additional channels of WV-2 (coastal blue, yellow, red edge and NIR2) were also performed.

For simplicity, and to avoid redundancy, the Kappa coefficient values are not included in Tables 3 and 5, but the same conclusions can be derived by using the overall accuracy.

To better analyze the previous results, Fig. 7 shows the mean overall accuracy for each sensor, ROI type and algorithm. As expected, accuracy mostly increases as the number of training pixels increases. We can observe that ultra-high resolution, as provided by the Pika-L, offers an excess of fine detail that implies greater variability in each class degrading the classification performance. Furthermore, the use of hyperspectral data does not demonstrate a clear benefit over multispectral information as very few bands reach the seafloor.

In general, SVM obtains higher accuracies but the simpler ML also provides satisfactory results. We can conclude that WorldView-2 can be the most appropriate sensor in this scenario.

Table 4 includes the computation times for each experiment. SVM clearly requires higher processing times than ML
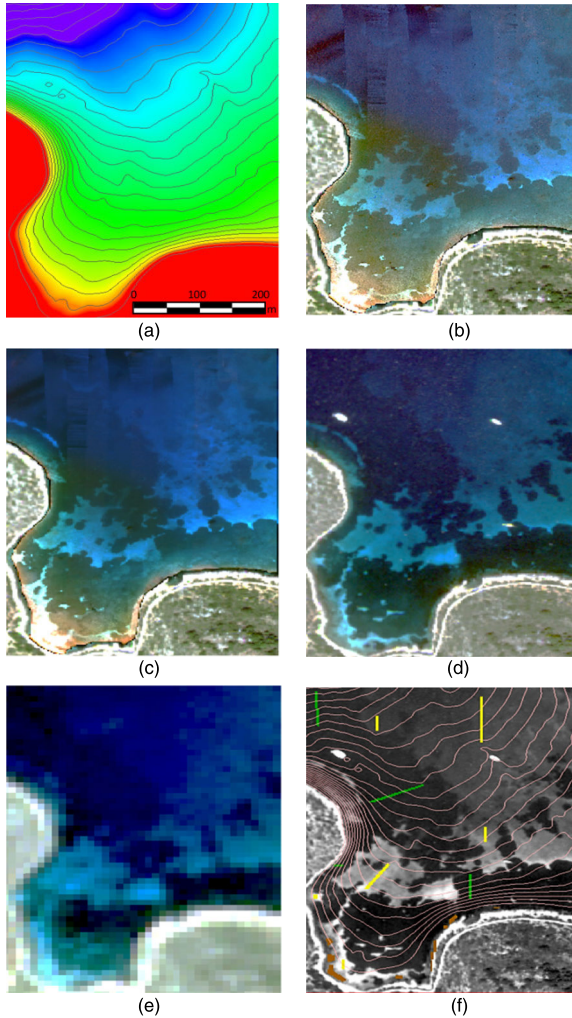
FIGURE 6. (a) Bathymetry with 1 m isobaths; (b) Pika-L 10 cm; (c) Pika-L 2 m; (d) WV-2; (e) S-2; (f) WV-2 (blue channel) with one example of ROI with an average number of pixels (200 pixels/class for a 2 m resolution).
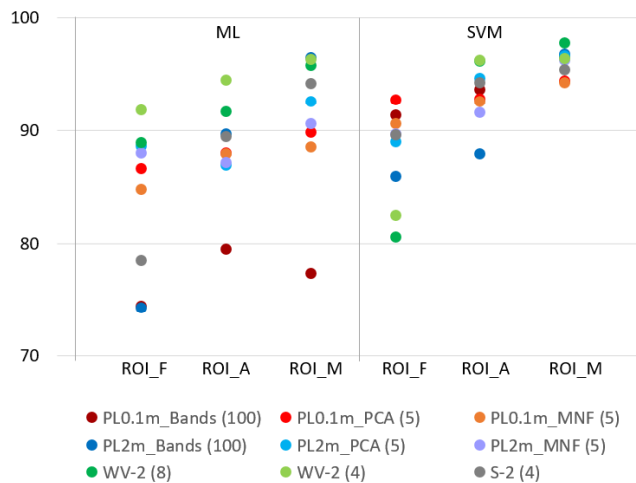
FIGURE 7. Mean overall accuracy for each sensor and ROI category using maximum likelihood and support vector machine algorithms.

and times increase dramatically for the hyperspectral image at the maximum resolution. PCA and MNF transforms can reduce them without loss of performance.

To improve classifications accuracy, further experiments including additional features have been carried out. Given the previous results (Table 3 and Fig. 7) only the ROI_M dataset has been considered. In particular, texture and bathymetric information were included in the analysis. Table 5 presents the overall accuracies (mean and standard deviation) for the different sensors and feature combinations, training ML and SVM algorithms with the ROI_M dataset. We can conclude that texture and bathymetry increase accuracy slightly, but only in some cases and mostly for the SVM classifier.

Fig. 8 shows the benthic maps obtained for each dataset, ML (left) and SVM (right), using the best combination from Table 5. A majority filter with a 3 × 3 kernel has been applied to remove isolated noisy pixels. In general, we can note that similar maps are derived for each type of imagery irrespective of their spectral and spatial resolutions, except the upper-left part of the RPAS scene due to sensing problems during the acquisition. Maps properly match the reference maps included in Fig.4.

B. MOUNTAIN ECOSYSTEM
The Teide National Park has been chosen as a high mountain area for its complexity and variability, as it is strongly stressed by climate change, herbivory pressure and tourism. Classifying the species is very challenging with remote sensing techniques as this shrubland ecosystem is mainly made up of small and mixed plant species (Fig 1(c)). For this reason, Sentinel-2 was not used as it cannot provide the appropriate spatial resolution.

The methodology presented in Fig. 5 has been applied to the MS and HS imagery provided by the 3 different platforms for the Teide National Park.

Table 6 shows the overall accuracy and Kappa coefficient of the vegetation maps generated by the SVM classifier. To properly compare results, the area covered by the RPAS in the northern part of the park has been selected for the study and the same training and test datasets have been used. For WorldView-2 imagery, apart from the original multispectral bands, the assessment has included the pansharpened data at 0.5 m applying the Gram-Schmidt (GS) algorithm. For the hyperspectral imagery, in addition to the original bands, the first 10 components of the MNF transformation have also been selected to retrieve the vegetation maps.

It can be appreciated that the 2 m (original WV-2 MS resolution) is not enough to accurately analyze this complex scene made up of small and mixed plant species. Conversely, resolutions under one meter can properly discriminate the different species. On the other hand, the MNF transform increases performance avoiding the so-called Hughes phenomenon in hyperspectral imagery when the amount of training samples is limited.

As accuracy is very similar for all the sensors, the most appropriate platform to generate the vegetation maps, factoring in cost, coverage and accuracy, is WorldView but after applying pansharpening techniques.

TABLE 3. Overall accuracy (%) of ML and SVM for the different sensors, input combinations and training datasets (Best accuracies for each classifier and ROI are marked in bold).

Platform	Input	ML			SVM		
		ROI_F	ROI_A	ROI_M	ROI_F	ROI_A	ROI_M
Pika-L	10cm_Bands (100)	74.5 ± 5.8	79.5 ±4.4	77.4 ±4.1	91.4 ±1.2	93.6 ±1.4	96.7 ±1.6
	10cm_PCA (5)	86.6 ±2.5	88.0 ±2.1	89.8 ±1.8	**92.7 ±1.4**	92.8 ±1.3	95.4 ±1.9
	10cm_MNF (5)	84.8 ±3.9	87.9 ±2.3	88.5 ±2.6	90.6 ±1.9	92.6 ±1.4	95.3 ±1.0
	2m_Bands (100)	74.3 ±6.9	89.7 ±4.4	**96.5 ±0.7**	85.9 ±0.5	87.9 ±2.5	96.8 ±0.7
	2m_PCA (5)	88.6 ±3.7	86.9 ±1.4	92.6 ±1.7	89.0 ±2.7	94.7 ±1.7	96.6 ±0.5
	2m_MNF (5)	88.0 ±3.6	87.1 ±4.8	90.6 ±3.0	89.6 ±2.8	91.6 ±3.0	96.3 ±1.2
WV-2	Bands (8)	88.9 ±4.5	91.7 ±5.4	95.8 ±1.7	80.5 ±2.0	96.2 ±1.4	**97.8 ±0.9**
	Bands B-G-R-NIR1 (4)	**91.8 ±3.1**	**94.5 ±1.2**	96.3 ±2.0	82.5 ±4.5	**96.3 ±0.8**	96.4 ±2.1
Sentinel-2	10m_Bands (4)	78.5 ±3.9	89.4 ±3.5	94.2 ±1.2	89.6 ±3.3	94.2 ±1.1	95.4 ±1.2

TABLE 4. Computation time for ML and SVM classifiers. Time is expressed in seconds, except in minutes or hours when indicated (ENVI 5.3 has been used in a laptop with Intel Core i7-7500U CPU 2.9 GHz, 8 GB of RAM and Windows-10 64 bits operating system).

Platform	Input	ML			SVM		
		ROI_F	ROI_A	ROI_M	ROI_F	ROI_A	ROI_M
Pika-L	10cm_Bands (100)	3.99 min	4.06 min	4.25 min	1.28 hr	4.02 hr	48.16 hr
	10cm_PCA (5)	16.73	17.33	18.44	0.62 hr	1.20 hr	25.56 hr
	10cm_MNF (5)	16.70	17.36	18.39	0.65 hr	1.31 hr	25.16 hr
	2m_Bands (100)	1.17	2.49	2.81	2.40	3.93	14.53
	2m_PCA (5)	0.78	0.92	1.11	1.35	2.23	4.64
	2m_MNF (5)	0.76	0.87	1.05	1.31	2.19	4.55
WV-2	Bands (8)	1.12	2.03	2.38	1.64	2.59	6.79
Sentinel-2	10m_Bands (4)	1.07	1.31	1.55	1.38	1.44	2.66

TABLE 5. Overall accuracy (%) of ML and SVM for the different sensors and input combinations including texture and bathymetry (Best accuracies marked in bold). B: Bands, T: Texture, Bath: Bathymetry.

Platform	Input	ML ROI_M	SVM ROI_M
Pika-L 10 cm	B (100)	77.40 ±4.08	96.66 ±1.59
	B+T (102)	77.42 ±3.92	**97.99 ±2.15**
	B+Bath (101)	78.64 ±4.50	97.93 ±2.67
	B+T+Bath (103)	**78.87 ±4.26**	97.91 ±2.99
Pika-L 2 m	B (100)	**96.51 ±0.70**	96.86 ±0.71
	B+T (102)	96.34 ±0.77	**97.13 ±0.95**
	B+Bath (101)	96.38 ±1.12	96.70 ±0.58
	B+T+Bath (103)	96.37 ±0.94	96.81 ±0.58
WV-2	B (8)	95.80 ±1.65	97.80 ±0.86
	B+T (10)	**96.43 ±1.01**	97.81 ±0.81
	B+Bath (9)	95.85 ±1.79	**97.99 ±0.77**
	B+T+Bath (11)	96.42 ±1.34	97.93 ±0.72
S-2	B (4)	**94.17 ±1.20**	95.43 ±1.23
	B+T (6)	93.46 ±1.16	96.03 ±0.90
	B+Bath (5)	93.94 ±2.61	97.39 ±1.07
	B+T+Bath (7)	94.06 ±1.68	**97.51 ±0.60**

TABLE 6. Overall accuracy (%) and Kappa coefficient of the SVM maps for the different sensors and combinations.

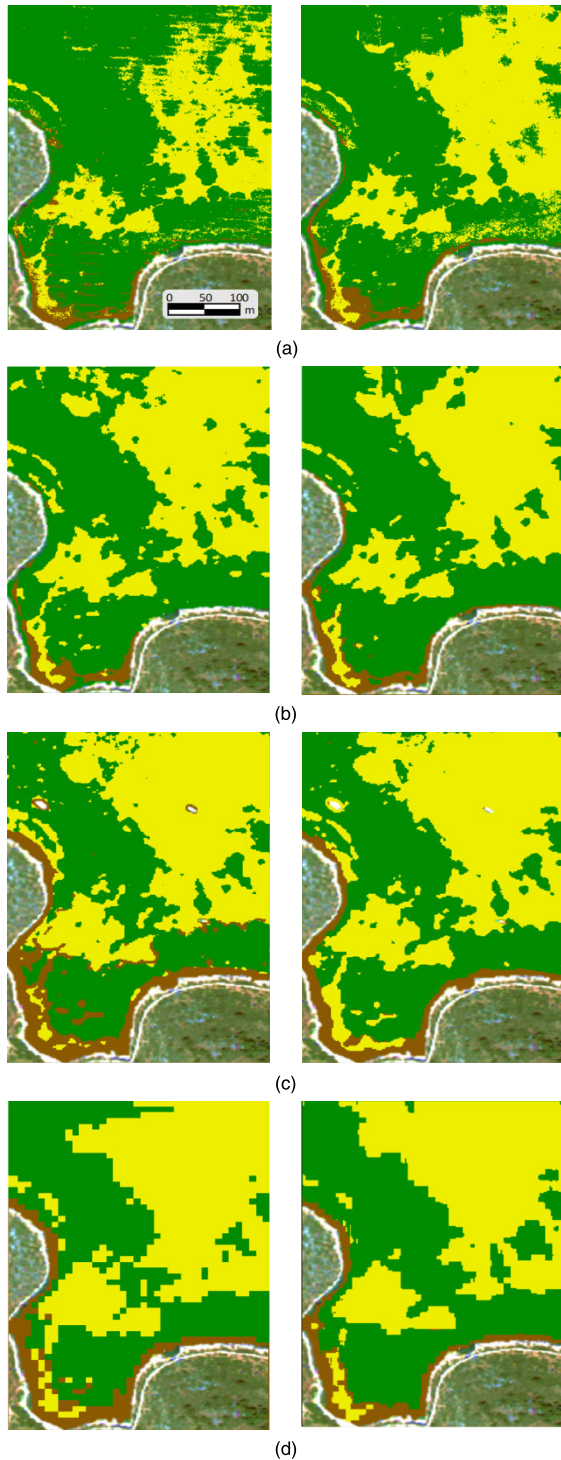| Platforms	WorldView-2		CASI		Pika-L	
	MS	GS	HS	MNF 10	HS	MNF 10
OA (%)	90.25	96.63	94.25	97.38	96.55	97.12
Kappa	0.870	0.953	0.914	0.960	0.933	0.944

spectral separability, the main limiting factor to get excellent performance is the spatial resolution.

Figs. 10 and 11 show the best vegetation maps for the northern part of the Park and a zoom of the scene, respectively. The radiometric problem in each strip sensed by the RPAS can be appreciated. In general, maps are similar but the higher spatial resolution of the Pika-L sensor allows the detection of more individuals of *D. bourgaeana* (Fig. 11).
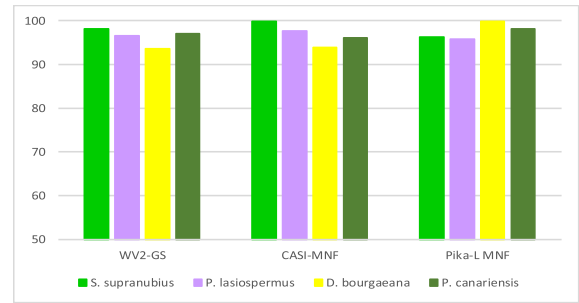
IV. DISCUSSION
A. PREPROCESSING
The development of new remote sensing platforms, with advanced imagery sensors and improved capabilities, can contribute to the conservation of natural resources in natural ecosystems. However, the data acquired by these sensors must be processed to properly extract accurate information. Appropriate correction algorithms are important to estimate reflectance information at surface level.

In particular, radiometric corrections are critical when using satellite to monitor coastal areas, as radiation reaching the sensor from the seafloor is very low due to the water column attenuation. Thus, the atmosphere severely

Analyzing the confusion matrix for each sensor's best map, and focusing on the plant species, it can be appreciated in Fig. 9 that results are mainly satisfactory. Spectral signatures have also been included to show the mean reflectance of each species with respect to wavelengths.

In summary, for this heterogeneous ecosystem, given the appropriate date of acquisition is chosen for the maximum
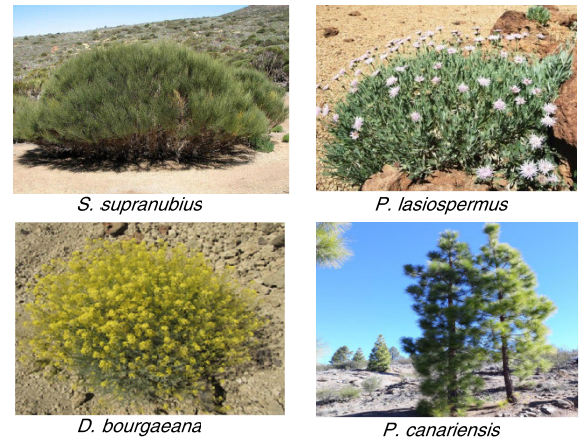
FIGURE 8. Best classification maps combining bands, texture or bathymetry for the Maximum Likelihood (left) and Support Vector Machine (right) classifiers: (a) Pika-L 10 cm.(b) Pika-L 2m. (c) WV-2.(d) S-2.

FIGURE 9. (a) Overall accuracy (%) of each plant species: WV-2 (50 cm); CASI (75 cm) and Pika-L (10 cm). (b) Field photo of the analyzed plant species. (c) Spectral signatures (mean value of the reflectance) measured by the ASD FieldSpec-3 field spectroradiometer.
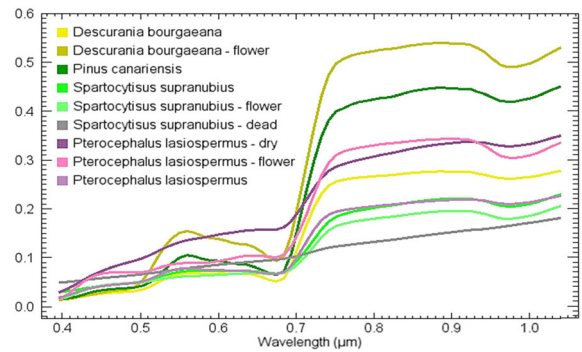
disturbs the sensed signal. To alleviate the atmospheric effects, different approaches have been developed [39], [40], mainly image-based correction techniques (DOS, COST, QUAC, etc.) and more complex radiative transfer models (MODTRAN, FLAASH, ATCOR, 6S, Sen2Cor, etc.).

As analyzed in previous works [6], [36], [41], different strategies have been compared with WorldView-2 data and, in general, radiative models properly remove the atmospheric contribution. In particular, FLAASH and 6S demonstrate excellent performance with low RMSE values in both coastal and vegetation zones.

RPAS imagery also requires important pre-processing tasks. Apart from the radiometric corrections, geometrics transforms are important to correct, orthorectify, co-register and generate the mosaic image from the individual strips. In mountain areas, a very high resolution digital elevation model is required while for coastal areas the bathymetric map is key to generating the composite image from the corrected strips.
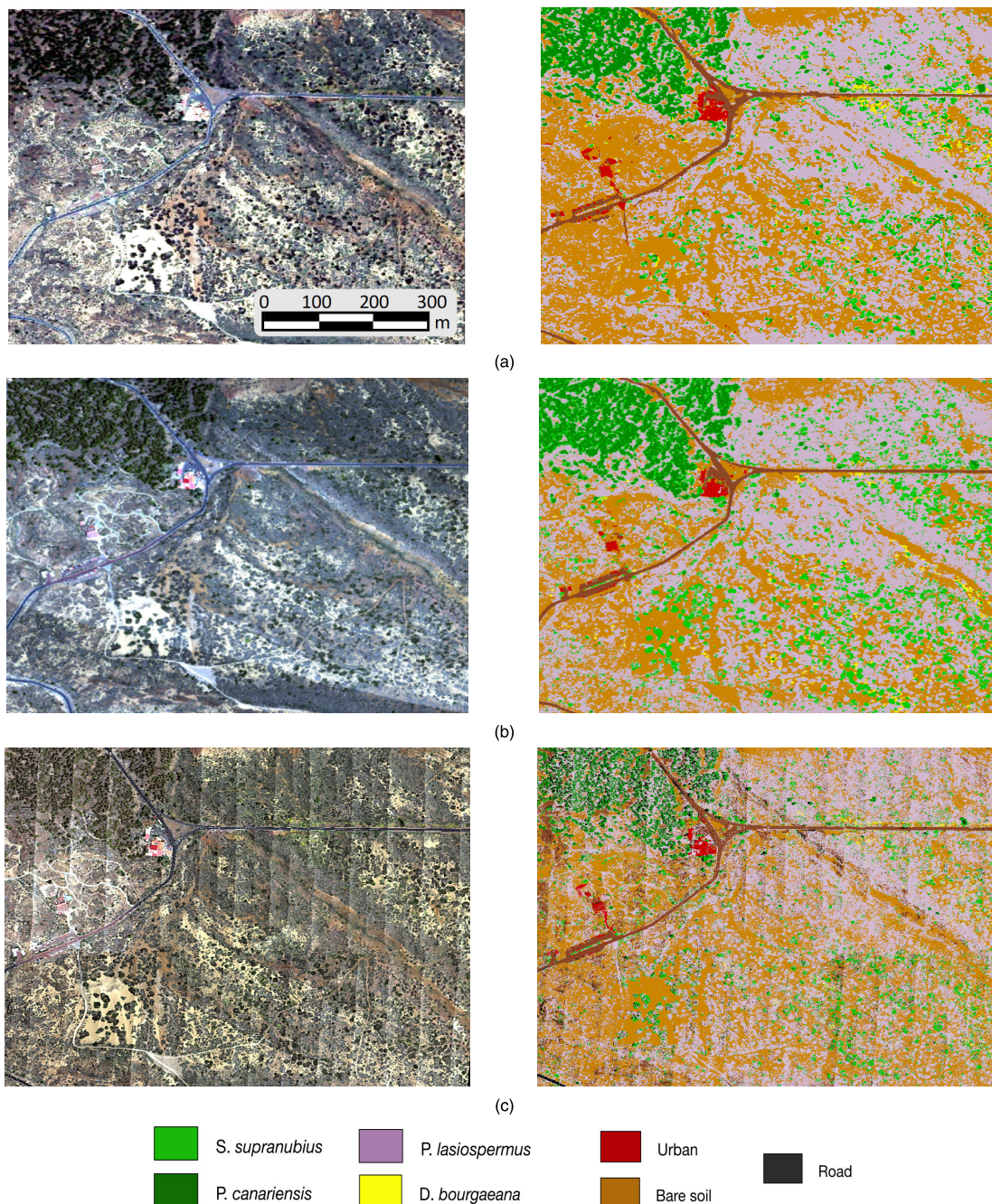
FIGURE 10. Best Support Vector Machine vegetation maps for each sensor: (a) WV-2 pansharpened GS. (b) CASI with 10 MNF components. (c) Pika-L with 10 MNF components.

B. COASTAL MONITORING

A comprehensive analysis of different features and processing techniques has been performed to obtain a robust methodology to produce the accurate benthic habitat maps. To select the best methods, different dimensionality reduction and feature extraction methods were assessed (Principal Component Analysis, Minimum Noise Fraction, Co-ocurrence matrix, etc.) as well as some supervised classification algorithms (Maximum Likelihood and Support Vector Machine).

Regarding the spatial resolution, the ultra-high resolution of Pika-L does not improve mapping results. Such fine detail makes classification more difficult. In fact, Pika-L with 2 m resolution improves, in general, the overall accuracy. For the considered scenario and the benthic classes to be discriminated, from the 3 different resolutions assessed (10 cm, 2 m and 10 m), 2m provides the highest accuracy. Specifically, WV-2 reaches an overall accuracy of 97.8% using SVM.

Concerning the spectral resolution, hyperspectral data does not provide a clear benefit over multispectral. In particular, comparing Pika-L and WorldView-2, both at the same spatial resolution, the multispectral data is more accurate in the
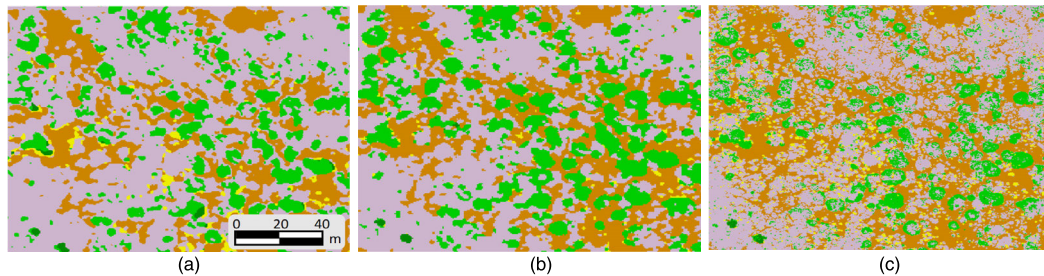
FIGURE 11. Zoom of an area of the SVM maps of Figure 10 (the same legend of colors applies): (a) WV-2 pansharpened GS. (b) CASI with 10 MNF components. (c) Pika-L with 10 MNF components.

majority of experiments performed. On the other hand, similar accuracies are reached for WorldView-2 using SVM with either 8 or 4 bands, and even better results using 4 bands with the ML classifier. Actually, very few bands reach the seafloor and the coastal blue of WV-2 is much noisier than the blue channel. On the other hand, dimensionality reduction transforms have demonstrated similar or even better classification performances, as in previous studies [5], [7] and with faster computation times.

Regarding the sensors, WorldView-2 has demonstrated, in general, a superior performance. The RPAS platform equipped with the hyperspectral sensor generates good maps but does not provide the best accuracy. Finally, Sentinel-2 is a good choice if it is not necessary to precisely outline the *Posidonia* meadows, providing the capability to get open and periodic imagery.

The analysis of the classification algorithms demonstrates that ML and SVM perform properly, although SVM achieves higher accuracies for all the sensors and ROIs datasets. Actually, results are similar except for the ROI with very few training pixels. It can be noted that ML classifier performance is more dependent on the training ROIs since the standard deviation is greater, indicating major differences in accuracy when the classification is repeated with different training areas. On average, for the 18 ROIs used, the variability (standard deviation) of ML is approximately twice that of SVM (3.3 vs. 1.7).

In any case, different factors affect the accuracy of seagrass mapping using remote sensing like: cloud cover, wind speed, sun angle, secchi depth, etc. [9]. Therefore, if possible, optimal conditions should be selected for the imagery acquisition.

C. MOUNTAIN MONITORING

The Teide National Park faces important challenges. The most relevant is the drop in the S. *supranubius* population, as a result of a rise in temperatures, drought episodes, and the growth in the rabbit populations [42]. Remote sensing can provide key information to analyze the conservation status of this area.

In general, the accuracy obtained by the satellite multispectral data and the hyperspectral airborne and RPAS imagery is excellent and very similar, highlighting the minor relevance

of having a large number of channels if the appropriate date is selected (May/June) and provided that the pixel size is less than one meter. The Pika-L image should have achieved the highest accuracy; however, the difficulty to properly mosaic all the image strips and the radiometric differences between them, due to changes in solar radiation caused by clouds, meant a slight decrease in performance. In summary, the most appropriate platform to generate the vegetation maps, taking into account cost, coverage and accuracy, is the WorldView-2 platform applying pansharpening techniques. Certainly, if WorldView-3 imagery is available it would be a better choice, taking into account the improved resolution of the panchromatic (31 cm) and multispectral bands (1.24 m). Worldview imagery is not free but its cost is affordable to cover areas of tens or hundreds of square kilometers.

Fig. 9 demonstrates that higher classification errors for WorldView-2 and CASI are due to D. *bourgaeana* because of its small size and low density that, mainly, means a misclassification with soil pixels. In fact, when these limiting factors (size and density) are not affecting, as for the Pika-L data, classification accuracy is highest. The remaining species are, in general, properly discriminated by all the platforms. Actually, according to the separability analysis performed during the training phase, the pairs of plant species with worst spectral separability were *P. canariensis – S. supranubius* and *S. supranubius – P. lasiospermus*. In any case, even for the WorldView-2 sensor, which has the worse spectral and spatial resolutions, the Jeffries-Matusita distance [43] for these pairs is quite good, with values over 1.9 (a perfect separability is 2).

It is important to emphasize the great climatic and spatial variability of the Park, due to its topography, where, for the selected date, the same plant species can be in different phenological phases (leafing, flowering, senesce). This fact makes the mapping process very challenging due to the significant variations in the spectral signatures, as it can be appreciated in Fig. 9(c). Accordingly, unmixing techniques were not suitable, even those using advanced algorithms that take into account the endmembers spectral variability.

Finally, it is worth mentioning that the main limitation in the use of SVMs is the need to select the suitable parameter values in order to improve its accuracy. Critical parameters for the Gaussian kernel are gamma (γ) and the

penalty (C) that controls the trade-off between allowing training errors and forcing rigid margins. Unfortunately, the best values are not known beforehand and, usually, a "grid-search" using cross-validation is applied to select them, first considering a coarse grid followed by a refined search around the former optimal parameters. Default values can be applied (γ = inverse of the number of bands and C = 100) with good results but, if an additional improvement is desired, this time consuming optimization procedure has to be carried out. Random Forest could be an alternative machine learning classifier that provides similar accuracy, but SVM usually achieves superior accuracy for the classification of hyperspectral and multispectral images. Recently deep learning algorithms have gained the researchers' attention; however, they require a large amount of training data and the developed models remain highly context and sensor dependent. In addition, most of the pre-trained deep learning networks are limited to 3 input bands, and therefore are not directly applicable to hyperspectral imagery.

V. CONCLUSION

Seagrass meadows in coastal areas as well as endemic vegetation in mountain ecosystems have to be sustainably preserved. In this context, analyzing very high resolution multiplatform remote sensing imagery can be an essential monitoring tool for conservation managers.

In this work, a complete processing methodology for the mapping of *Posidonia oceanica* and high mountain vegetation has been developed to monitor coastal and mountain ecosystems. Multispectral and hyperspectral data recorded by satellite and airborne sensors have been used and the benefits and drawbacks of each technology identified. Advanced processing algorithms in each stage of the methodology have been carefully chosen to provide accurate benthic and vegetation maps. Results have been validated using in-situ measurements collected during field campaigns and by the Park managers.

In summary, the assessment has demonstrated the excellent performance of high resolution hyperspectral and multispectral imagery and, specifically, the WorldView-2 satellite, applying the appropriate correction, enhancement and classification techniques, can be a suitable sensor, providing a robust and systematic framework to monitor the status and variability of coastal and mountain areas.

Future studies will focus on analyzing changes using multitemporal imagery and on the application of deep learning techniques to generate benthic and vegetation maps.

ACKNOWLEDGMENT

REFERENCES

[1] UNEP-WCMC, IUCN and NGS. (2018). *Protected Planet Report*. Cambridge, U.K. [Online]. Available: https://livereport.protectedplanet. net/pdf/Protected_Planet_Report_2018.pdf

[2] M. C. Múgica Montes and C. Castell. (in Spanish), *Society and Protected Areas Program 2020. Protected Areas for Human Well-Being*, F. González and B. Madrid, Eds. [Online]. Available: http://www.redeuroparc. org/system/files/shared/Programa_2020/programa2020.pdf

[3] N. Pettorelli *et al.*, "Satellite remote sensing of ecosystem functions: Opportunities, challenges and way forward," *Remote Sens. Ecology Conservation*, vol. 4, no. 2, pp. 71–93, Aug. 2017.

[4] M. Chu and H. Zhang, "Comparison experiment of sun glint correction method for nearshore high-resolution multispectral satellite images," *Proc. SPIE*, vol. 10850, Dec. 2018, Art. no. 108500R.

[5] J. Marcello, F. Eugenio, J. Martín, and F. Marqués, "Seabed mapping in coastal shallow waters using high resolution multispectral and hyperspectral imagery," *Remote Sens.*, vol. 10, no. 8, p. 1208, Aug. 2018.

[6] F. Eugenio, J. Marcello, J. Martin, and D. Rodríguez-Esparragón, "Benthic habitat mapping using multispectral high-resolution imagery: Evaluation of shallow water atmospheric correction techniques," *Sensors*, vol. 17, no. 11, p. 2639, Nov. 2017.

[7] P. Wicaksono, "Improving the accuracy of multispectral-based benthic habitats mapping using image rotations: The application of principle component analysis and independent component analysis," *Eur. J. Remote Sens.*, vol. 49, no. 1, pp. 433–463, Feb. 2017.

[8] Li, Fabina, Knapp, and Asner, "The sensitivity of multi-spectral satellite sensors to benthic habitat change," *Remote Sens.*, vol. 12, no. 3, p. 532, Feb. 2020.

[9] N. K. Nahirnick, L. Reshitnyk, M. Campbell, M. Hessing-Lewis, M. Costa, J. Yakimishyn, and L. Lee, "Mapping with confidence; delineating seagrass habitats using unoccupied aerial systems (UAS)," *Remote Sens. Ecology Conservation*, vol. 5, no. 2, pp. 121–135, Nov. 2018.

[10] A. M. Machín, J. Marcello, A. I. Hernández-Cordero, J. M. Abasolo, and F. Eugenio, "Vegetation species mapping in a coastal-dune ecosystem using high resolution satellite imagery," *GISci. Remote Sens.*, vol. 56, no. 2, pp. 210–232, Feb. 2019.

[11] E. Ibarrola-Ulzurrun, J. Marcello, C. Gonzalo-Martín, and J. L. Martín-Esquivel, "Temporal dynamic analysis of a mountain ecosystem based on multi-source and multi-scale remote sensing data," *Ecosphere*, vol. 10, no. 6, Jun. 2019.

[12] P. Wicaksono, P. A. Aryaguna, and W. Lazuardi, "Benthic habitat mapping model and cross validation using machine-learning classification algorithms," *Remote Sens.*, vol. 11, no. 11, p. 1279, May 2019.

[13] E. Kovacs, C. Roelfsema, M. Lyons, S. Zhao, and S. Phinn, "Seagrass habitat mapping: How do landsat 8 OLI, sentinel-2, ZY-3A, and Worldview-3 perform?" *Remote Sens. Lett.*, vol. 9, no. 7, pp. 686–695, Jul. 2018.

[14] T. T. Sankey, J. McVay, T. L. Swetnam, M. P. McClaran, P. Heilman, and M. Nichols, "UAV hyperspectral and lidar data and their fusion for arid and semi-arid land vegetation monitoring," *Remote Sens. Ecology Conservation*, vol. 4, no. 1, pp. 20–33, Apr. 2017.

[15] S. Purkis, and V. Klemas, *Remote Sensing and Global Environmental Change*. Hoboken, NJ, USA: Wiley, 2011.

[16] N. Horning, J. A. Robinson, E. J. Sterling, W. Turner, and S. Spector, *Techniques in Ecology & Conservation*. London, U.K.: Oxford Univ. Press, 2010.

[17] *BOIB. Decree 25/2018 of July 27 on the conservation of Posidonia in the Balearic Islands. Official bulletin of the Balearic Islands n° 93*, document Fascicle 130-Sec I, 2018, pp. 25994–26042.

[18] M. E. Arozena, and E. Beltran, "Geografía de la vegetación de las coladas domáticas del atrio de las Cañadas del Teide (Tenerife. I. Canarias)," in *Serie Geográfica-Biogeografía, Distribuciones, Dinámicas y Diversidad*. Madrid, Spain: Universidad de Alcalá de Henares, 2006.

[19] M. Main-Knorn, B. Pflug, J. Louis, V. Debaecker, U. Müller-Wilm, and F. Gascon, "Sen2Cor for Sentinel-2," *Proc. SPIE* vol. 10427, Oct. 2017, Art. no. 1042704.

[20] J. Martin, F. Eugenio, J. Marcello, and A. Medina, "Automatic sun glint removal of multispectral high-resolution Worldview-2 imagery for retrieving coastal shallow water parameters," *Remote Sens.*, vol. 8, no. 1, p. 37, Jan. 2016.

[21] F. Eugenio, J. Marcello, and J. Martin, "High-resolution maps of bathymetry and benthic habitats in shallow-water environments using multispectral remote sensing imagery," *IEEE Trans. Geosci. Remote Sens.*, vol. 53, no. 7, pp. 3539–3549, Jul. 2015.

[22] J. A. Richards, *Remote Sensing Digital Image Analysis*. 5th ed. Berlin, Germany: Springer, 2013.

[23] R. M. Haralick, K. Shanmugam, and I. Dinstein, "Textural features for image classification," *IEEE Trans. Syst., Man, Cybern.*, vol. SMC-3, no. 6, pp. 610–621, Nov. 1973.

[24] (2019). *IEO (Instituto Español de Oceanografía), Parque Nacional Marítimo-Terrestre del Archipiélago de Cabrera (Data Source)*. [Online]. Available: http://www.ideo-cabrera.ieo.es/

[25] P. Ghamisi, J. Plaza, Y. Chen, J. Li, and A. J. Plaza, "Advanced spectral classifiers for hyperspectral images: A review," *IEEE Geosci. Remote Sens. Mag.*, vol. 5, no. 1, pp. 8–32, Mar. 2017.

[26] U. Maulik and D. Chakraborty, "Remote sensing image classification: A survey of support-vector-machine-based advanced techniques," *IEEE Geosci. Remote Sens. Mag.*, vol. 5, no. 1, pp. 33–52, Mar. 2017.

[27] G. Mountrakis, J. Im, and C. Ogole, "Support vector machines in remote sensing: A review," *ISPRS J. Photogramm. Remote Sens.*, vol. 66, no. 3, pp. 247–259, May 2011.

[28] M. J. Canty, *Image Analysis, Classification, and Change Detection in Remote Sensing: With Algorithms for ENVI/IDL*. 2nd ed. Boca Raton, FL, USA: CRC Press, 2010.

[29] *LIFE Posidonia Project 00/NAT/E/7303, Cartografía de Posidonia Oceanica en LICs de Balears. Mapa de Cabrera*, Balearic Islands Government, Local Ministry Environ., Palma, Spain, 2015.

[30] G. Vivone, L. Alparone, J. Chanussot, M. Dalla Mura, A. Garzelli, G. A. Licciardi, R. Restaino, and L. Wald, "A critical comparison among pansharpening algorithms," *IEEE Trans. Geosci. Remote Sens.*, vol. 53, no. 5, pp. 2565–2586, May 2015.

[31] E. Ibarrola-Ulzurrun, C. Gonzalo-Martín, and J. Marcello, "Influence of pansharpening in obtaining accurate vegetation maps," *Can. J. Remote Sens.*, vol. 43, no. 6, pp. 528–544, Sep. 2017.

[32] J. Marcello, E. Ibarrola-Ulzurrun, C. Gonzalo-Martin, J. Chanussot, and G. Vivone, "Assessment of hyperspectral sharpening methods for the monitoring of natural areas using multiplatform remote sensing imagery," *IEEE Trans. Geosci. Remote Sens.*, vol. 57, no. 10, pp. 8208–8222, Oct. 2019.

[33] H. Wu, S. Zhao, J. Zhang, and C. Lu, "Remote sensing image sharpening by integrating multispectral image super-resolution and convolutional sparse representation fusion," *IEEE Access*, vol. 7, pp. 46562–46574, 2019.

[34] C. A. Laben and B. V. Brower, "Process for enhancing the spatial resolution of multispectral imagery using pan-sharpening," U.S. Patent 6 011 875 A, Jan. 4, 2000.

[35] T. Cooley, G. P. Anderson, G. W. Felde, M. L. Hoke, A. J. Ratkowski, J. H. Chetwynd, J. A. Gardner, S. M. Adler-Golden, M. W. Matthew, A. Berk, L. S. Bernstein, P. K. Acharya, D. Miller, and P. Lewis, "FLAASH, a MODTRAN4-based atmospheric correction algorithm, its application and validation," in *Proc. IEEE Int. Geosci. Remote Sens. Symp.*, Jun. 2002, pp. 1414–1418.

[36] J. Marcello, F. Eugenio, U. Perdomo, and A. Medina, "Assessment of atmospheric algorithms to retrieve vegetation in natural protected areas using multispectral high resolution imagery," *Sensors*, vol. 16, no. 10, p. 1624, Sep. 2016.

[37] G. Hughes, "On the mean accuracy of statistical pattern recognizers," *IEEE Trans. Inf. Theory*, vol. IT-14, no. 1, pp. 55–63, Jan. 1968.

[38] E. Ibarrola-Ulzurrun, J. Marcello, and C. Gonzalo-Martin, "Assessment of component selection strategies in hyperspectral imagery," *Entropy*, vol. 19, no. 12, p. 666, Dec. 2017.

[39] E. J. Ientilucci and S. Adler-Golden, "Atmospheric compensation of hyperspectral data: An overview and review of in-scene and physics-based approaches," *IEEE Geosci. Remote Sens. Mag.*, vol. 7, no. 2, pp. 31–50, Jun. 2019.

[40] R. Pu, S. Landry, and J. Zhang, "Evaluation of atmospheric correction methods in identifying urban tree species with WorldView-2 imagery," *IEEE J. Sel. Topics Appl. Earth Observ. Remote Sens.*, vol. 8, no. 5, pp. 1886–1897, May 2015.

[41] F. Eugenio, J. Marcello, and J. Martín, "Multiplatform Earth observation systems for monitoring water quality in vulnerable inland ecosystems: Maspalomas water lagoon," *Remote Sens.*, vol. 12, no. 2, p. 284, Jan. 2020.

[42] J. Cubas, J. L. Martín-Esquivel, M. Nogales, S. D. H. Irl, R. Hernández-Hernández, M. López-Darias, M. Marrero-Gómez, M. J. del Arco, and J. M. González-Mancebo, "Contrasting effects of invasive rabbits on endemic plants driving vegetation change in a subtropical alpine insular environment," *Biol. Invasions*, vol. 20, no. 3, pp. 793–807, Mar. 2018.

[43] B. Tso, and P. Mather, *Classification Methods for Remotely Sensed Data*. 2nd ed. Boca Raton, FL, USA: CRC Press, 2009.

JAVIER MARCELLO (Senior Member, IEEE) received the M.S. degree in electrical engineering from the Technical University of Catalonia, Barcelona, Spain, in 1993, and the Ph.D. degree from the Universidad de Las Palmas de Gran Canaria (ULPGC), Las Palmas de Gran Canaria, Spain, in 2006.

From 1992 to 2000, he was the Head Engineer with the Canary Space Center, INTA, Spanish Aerospace Defense Administration. In 1994, he joined the Department of Signal and Communications, ULPGC, where he has been an Associate Professor with the Telecommunication School, lecturing on the areas of satellite and radio communications, since 2000. His research is carried out at the Institute of Oceanography and Global Change, ULPGC. He has authored more than 30 articles in remote sensing journals with medium–high impact factor. His research interests include multisensor remote sensing image processing and the generation of coastal and land products.

Dr. Marcello has been the Vice-President of the IEEE Geoscience and Remote Sensing Spanish Chapter since 2016. He has also served as a reviewer of more than 25 remote sensing publications.

FRANCISCO EUGENIO (Senior Member, IEEE) received the B.S., M.S., and Ph.D. degrees from the University of Las Palmas of Gran Canaria (ULPGC), Las Palmas, in 1986, 1993, and 2000, respectively, all in electrical engineering. He joined the Department of Signal and Communications, ULPGC, in 1996. From 1997 to 2000, he was with the Universitat Politecnica de Catalunya, Barcelona. He served as the Dean with the School of Electrical Engineering, ULPGC, from 2004 to 2010, where he is currently a Professor. His research is carried out at the Institute of Oceanography and Global Change, ULPGC. His current research interests include remote sensing image processing focuses on new methodologies/algorithms for multispectral/hyperspectral high-resolution multiplatform remote sensing imagery for the monitoring of shallow-waters and inland natural ecosystems. In these areas, he has authored or coauthored many publications that have appeared as journal articles and proceeding articles.

CONSUELO GONZALO-MARTÍN received the Ph.D. degree in physics from the Complutense University of Madrid in 1989. Since 1991, she has been with the Computer School of Universidad Politécnica de Madrid (UPM). Since 2012, she has been carrying out her research activities with the Center for Biomedical Technology, UPM. Her main contributions have been in the areas of image processing and the development of new artificial neural networks algorithms in remote sensing, medical imaging, and recognition of faces. Her current main line of research is new methodologies for image analysis based on objects for satellite images and medical images. She is also involved in text and image mining in the health care domain.

DIONISIO RODRÍGUEZ-ESPARRAGÓN received the B.Sc. degree in telecommunications engineering from the Universidad de Las Palmas de Gran Canaria, in 1990, the M.Sc. degree in mathematics from the Universidad de Granada, in 2010, and the Ph.D. degree in cybernetics and telecommunications from the Universidad de Las Palmas de Gran Canaria, in 2016. He joined the Departamento de Señales y Comunicaciones, Universidad de Las Palmas de Gran Canaria, in 1990, where he is currently an Assistant Professor. His current research interest includes processing of high-resolution remote sensing imagery.

FERRAN MARQUÉS (Senior Member, IEEE) received the degree in electrical engineering and the Ph.D. degree from the Universitat Politecnica de Catalunya, BarcelonaTech (UPC), where he is currently a Professor with the Department of Signal Theory and Communications. From 2002 to 2004, he served as the President of the European Association for Signal Processing (EURASIP).

He has served as the Dean with the Electrical Engineering School (ETSETB-TelecomBCN), UPC, from 2012 to 2019. He has authored or coauthored over 150 conference and journal papers and two books. He holds four international patents. In 2011, he received the Jaume Vicens Vives distinction for University Teaching Quality. He has served as Associate Editor for the IEEE Transactions on Image Processing from 2009 to 2012 and an Area Editor for *Signal Processing: Image Communication* (Elsevier) from 2010 to 2014.

● ● ●